

## Transition metal NMR spectroscopy—a probe into organometallic structure and catalysis\*

Wolfgang von Philipsborn

Department of Chemistry, University of Zurich, Switzerland

**Abstract** - Significant advances in NMR detection of insensitive, low-frequency spin-1/2 and quadrupolar nuclei have caused rapid progress in the application of transition metal NMR spectroscopy to organometallic chemistry. As a result, the structural dependence of metal NMR parameters, i.e. chemical shifts, heteronuclear and homonuclear spin coupling and relaxation times, has become a topical field of research.

Following a survey of current detection methods, high-resolution and broad-line NMR spectra of  $^{57}\text{Fe}$ ,  $^{59}\text{Co}$  and  $^{103}\text{Rh}$  nuclei in mono- and dinuclear olefin complexes are discussed. Particular attention is given to structural effects on nuclear shielding in low-valent metal complexes, to metal-carbon spin coupling, stereoelectronic effects in p,d-bonding, charge distribution in dinuclear complexes, and to intramolecular dynamic processes.

For substituted CpCo(COD) and IndCo(COD) complexes quantitative correlations between  $^{59}\text{Co}$  shielding and the activity and regioselectivity in homogeneous catalysis of the pyridine synthesis permit a novel and effective screening of catalysts.

The first report on  $^{59}\text{Co}$ -NMR spectra of cobalamins (vitamin- $\text{B}_{12}$  and methylcobalamin) suggests potential applications in biocatalysis.

### INTRODUCTION

The thorough investigation of transition metal NMR spectroscopy of organometallic compounds was handicapped for a long time by a lack of sensitive detection techniques suitable to cover a wide range of resonance frequencies. During the past few years, the availability of high-field spectrometers, with provision for the use of large sample volumes in conjunction with broad-banded r.f. electronics and programmable pulse generators, has caused a real break-through in a field which may be considered of great potential for organometallic chemistry and homogeneous catalysis.

### METHODS

Experimental problems for the detection and routine measurement of transition metal resonances may arise from either of the following facts. First, very small magnetic moments lead to low Larmor frequencies and sensitivities and, for spin-1/2 nuclei, to rather long spin-lattice relaxation times, e.g.  $^{57}\text{Fe}$ ,  $^{103}\text{Rh}$ ,  $^{107}\text{Ag}/^{109}\text{Ag}$ . Second, nuclei with spin  $\geq 1$  may have large electric quadrupole moments (e.g.  $^{59}\text{Co}$ ,  $^{61}\text{Ni}$ ,  $^{105}\text{Pd}$ ) which cause extremely short nuclear relaxation times  $T_1$  and  $T_2$ , the latter being responsible for large experimental line width (up to 30 KHz). In addition, low natural isotope abundance may lead to detection problems due to very small over-all receptivity. The magnetic properties of some typical transition metals of major chemical importance are summarized in Table 1.

\* Transition metal NMR spectroscopy Part VIII, Part VII: ref. 1.

TABLE 1. NMR properties of group VIII metals

	<sup>57</sup> Fe	<sup>103</sup> Rh	<sup>195</sup> Pt	<sup>61</sup> Ni	<sup>59</sup> Co	<sup>105</sup> Pd
Frequency MHz, 9.4 T	12.9	12.6	86.0	35.7	94.5	18.3
% Isotope	2.2	100	33.7	1.2	100	22.2
Spin [ $\hbar$ ]	1/2	1/2	1/2	3/2	7/2	5/2
Sensitivity <sup>13</sup> C: 1.0	0.002	0.002	0.62	0.23	17.6	0.07
Receptivity	0.004	0.18	18.7	0.24	1590	1.4
Chemical Shift range	KHz ppm	150 12000	120 10000	1100 13000	? 1700 18000	? ?

Although in this account we will focus our attention on NMR spectra of some group VIII nuclei the following Table 2 is meant to illustrate the variety of methods nowadays available for the general detection of transition metals in organometallic compounds in the liquid state. The rather unexplored but also rapidly developing area of metal NMR of solids will not be discussed here.

TABLE 2. Detection methods for transition metals

I = 1/2 large $\gamma$ short $T_1$	<sup>111</sup> Cd, <sup>113</sup> Cd <sup>195</sup> Pt <sup>199</sup> Hg	normal pulse techniques at low or medium field strength $B_0$
I = 1/2 small $\gamma$ long $T_1$	<sup>57</sup> Fe <sup>103</sup> Rh <sup>109</sup> Ag <sup>187</sup> Os	normal pulse techniques at <u>high</u> fields steady state techniques at low fields polarization transfer (INEPT, DEPT) large sample volumes
I $\gg$ 1 small Q	<sup>63</sup> Cu, <sup>65</sup> Cu <sup>67</sup> Zn <sup>95</sup> Mo <sup>99</sup> Ru	normal pulse techniques
I $\gg$ 1 large Q short $T_2$	<sup>55</sup> Mn <sup>59</sup> Co <sup>61</sup> Ni <sup>105</sup> Pd	very fast pulsing AT 100 $\mu$ s - 1 ms high fields when receptivity low

It is evident that the main improvements for the measurement of low- $\gamma$  spin-1/2 nuclei arise from the application of high magnetic fields and pulse techniques causing polarization transfer from fast-relaxing and sensitive nuclei such as <sup>1</sup>H, <sup>19</sup>F or <sup>31</sup>P (ref. 2). In a field of  $B_0 = 9.4$  T spin lattice relaxation times (Table 4) are typically 1-20 sec for small olefin complexes of Fe and Rh, and thus conventional single-pulse techniques may be applied. At lower fields, e.g. 2.1 T corresponding to Larmor frequencies of 2.8 MHz for <sup>103</sup>Rh and 2.9 MHz for <sup>57</sup>Fe, only steady state pulse techniques have proven suitable for obtaining useful sensitivities despite very long relaxation times  $T_1$  (ref. 3, 4, 5). The considerable increase of sensitivity at high fields thus originates from its about linear dependence on  $B_0$  and a much more effective  $T_1$  relaxation (Table 4) due to significant chemical shift anisotropy contributions. For quadrupolar nuclei, both the sensitivity gain from higher fields and the increased spectral width of broad-banded r.f. electronics ( $\sim 170$  KHz) contribute to facilitate signal detection.

Spin-1/2 metal nuclei which show a significant spin coupling to an abundant high- $\gamma$  nucleus, e.g.  $^1\text{H}$ ,  $^{19}\text{F}$  or  $^{31}\text{P}$ , may be detected with much increased sensitivity by applying the INEPT (ref. 6) or DEPT (ref. 7) pulse sequences. The maximum signal enhancement factor for polarization transfer from protons is given by  $\gamma(\text{H})/\gamma(\text{M})$  which can be as large as 30 for low- $\gamma$  nuclei such as  $^{103}\text{Rh}$  or  $^{57}\text{Fe}$ .

As a result of these experimental improvements the NMR spectral parameters of transition metal nuclei are now more readily accessible, i.e. shielding values, heteronuclear and homonuclear spin coupling constants, and relaxation times. Their determination and application in structural studies has become a topical field of research and enables the chemist and biochemist to probe the reactive centre and dynamic behaviour of metal complexes.

## APPLICATIONS

### $^{57}\text{Fe}$ -NMR Studies

In continuation of our earlier studies on the geometry of transition metal complexed dienes, using high-resolution  $^1\text{H}$ - and  $^{13}\text{C}$ -NMR spectra (ref. 8, 9), we have investigated  $^{57}\text{Fe}$  chemical shifts in a large series of  $(\eta^4\text{-diene})\text{Fe}(\text{CO})_3$  complexes (ref. 4a) in order to determine in which way shielding of the metal nucleus is influenced by ligand geometry, substituents and heteroatoms in low-valent iron complexes. Figure 1 shows a typical  $^{57}\text{Fe}$  spectrum and illustrates the excellent sensitivity and resolution obtainable at 12.9 MHz and with 20 mm sample tubes in a 9.4 T wide-bore superconducting magnet.

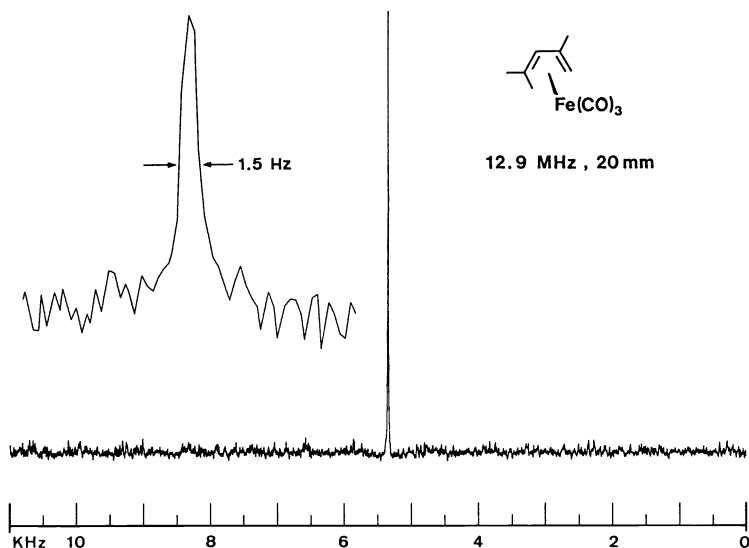


Fig. 1.  $^{57}\text{Fe}$ -NMR spectrum of  $(2,4\text{-dimethylpenta-1,3-diene})\text{Fe}(\text{CO})_3$ , 2.3 M in  $\text{C}_6\text{D}_6$ , total acquisition time 21 h. The signal is detectable after ca. 1 h,  $\delta(\text{Fe}) = 219.0$  ppm.

Iron chemical shifts are conveniently expressed relative to neat  $\text{Fe}(\text{CO})_5$  as an external reference at the low-frequency end of the scale (ref. 4a). Its resonance position is well known also as a function of temperature and solvent (ref. 4b). The  $\delta(\text{Fe})$  values of formally zero-valent iron complexes cover a range of about 1500 ppm whereby only a few compounds have as yet become known which appear at lower frequencies (i.e. neg.  $\delta$ -values) than the reference  $\text{Fe}(\text{CO})_5$ . The total chemical shift range of the  $^{57}\text{Fe}$  nucleus, as known to date, is illustrated in Fig. 2 and amounts to about 12'000 ppm, corresponding to 150 KHz at 12.9 MHz. It is apparent that the formal oxidation state of iron in organometallic and inorganic complexes determines the gross position on the shift scale, i.e.  $\text{Fe}(\text{II})$  at high frequencies,  $\text{Fe}(\text{0})$  at low frequencies and intermediate cases, such as the ferrocenes (ref. 10, 11) and cationic olefin complexes (ref. 4a) at intermediate positions. However, it should be noted that electronegative heteroatoms directly bound to the

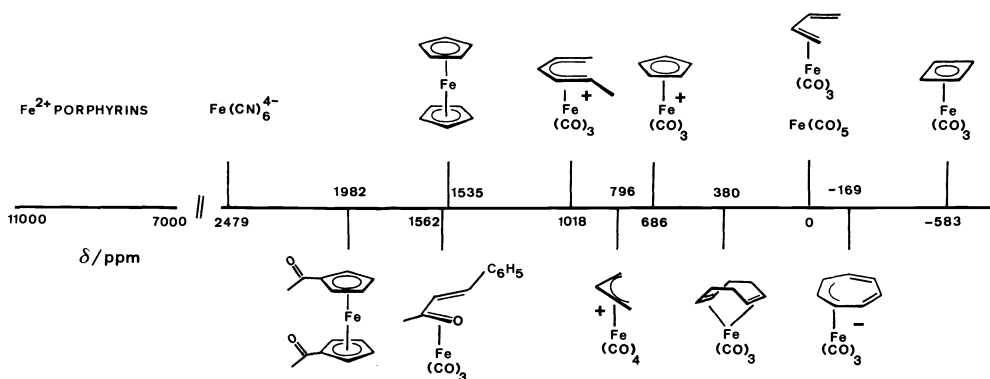
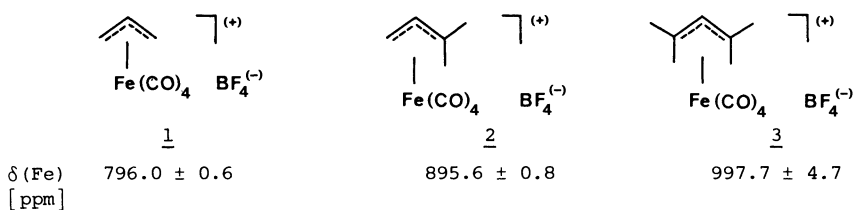


Fig. 2. Chemical shift range of the  $^{57}\text{Fe}$  nucleus, reference  $\text{Fe}(\text{CO})_5$

metal, e.g. in the iron(II) porphyrin complexes and in the 1-phenylbuten-3-one complex, cause additional large deshielding effects, as also observed with other transition metals, e.g. Co, Rh (ref. 12). Furthermore, it was reported that certain cationic organoiron complexes show rather high shielding values, for example protonated ferrocene and  $\alpha$ -ferrocenylcarbenium ions, relative to ferrocenes (ref. 10). These effects were ascribed to rehybridization of the iron non-bonding d-orbitals. Thus, a more detailed or even quantitative attempt to interpret iron chemical shifts must be based on a careful consideration of the various factors in the paramagnetic shielding term.


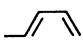
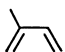
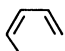

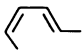
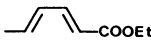
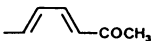
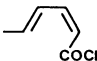
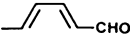
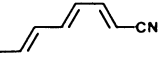
A successful, if only empirical, way out of these difficulties lies in the inspection of chemical shifts within a class of well-defined complexes and the systematic effects of substituents then become clearly visible. A well-studied example are variously substituted ( $\eta^4$ -diene) $\text{Fe}(\text{CO})_3$  complexes with open-chain and cyclic diolefin ligands (ref. 4a, 13). It was in this class of complexes that an interesting and apparently general shielding phenomenon for transition metal olefin complexes was observed for the first time, the subtle dependence of  $^{57}\text{Fe}$  shielding on diene geometry and steric effects of alkyl substituents. As seen from the data in Table 3, iron shielding decreases with increasing ring size of the 1,3-diene system and is generally lower in 1,4 and 1,5 diene systems. The cyclopentadiene complex, which may be considered as a 1,3- and 1,4-diene system, shows an intermediate chemical shift. Furthermore, terminal methyl substitution on the 1,3-butadiene ligand causes deshielding effects which are 3-4 times larger for a *cis*- than for a *trans*-methyl group (ref. 13). We will call these significant deshielding phenomena stereoelectronic effects since they may evolve from changes in  $p, \pi$ - $d, \pi$  overlap. We shall see in the chapter on  $^{59}\text{Co}$ -NMR for the series of  $\text{CpCo}(\text{diene})$  complexes that such deshielding effects of the metal resonance correlate with increasing thermal instability and catalytic activity of the complexes, a first and very significant discovery in these metal chemical shift studies. Similar stereoelectronic deshielding effects are observed in methyl-substituted  $[(\text{allyl})\text{Fe}(\text{CO})_4]^+$  ions, e.g. 2 and 3:

Scheme 1



Although this gem-dimethyl effect is large (+ 100 ppm) and additive, the substituent effects on the  $^{57}\text{Fe}$  resonance in cationic  $\eta^3$ -allyl systems are more complex than in  $\eta^4$ -diene systems, presumably due to the greater mobility of the coordinated allyl ligand. Also, an inductive effect leading to a shielding of the iron nucleus can be recognized, e.g. on introduction of a trans-methyl group at C(4) of complex 2 ( $884.0 \pm 1.4$  ppm). Such shielding effects are described also for methyl-substituted (Ind)Co(diene) complexes.

TABLE 3.  $^{57}\text{Fe}$  chemical shifts in (diene)Fe(CO) $_3$  complexes

diene	$\delta(\text{Fe})/\text{ppm}$	Solvent
cyclobutadiene	-583.2	$\text{C}_6\text{H}_6$
cyclohexa-1,3-diene	- 72.9	$\text{C}_6\text{D}_6$
cyclohepta-1,3-diene	+ 86.4	$\text{C}_6\text{H}_6$
cycloocta-1,3-diene	+169.4	$\text{C}_6\text{H}_6$
cyclopentadiene	+185.4	$\text{C}_6\text{H}_6$
norborna-1,4-diene	+382.0	$\text{C}_6\text{H}_6$
cycloocta-1,5-diene	+380.4	$\text{C}_6\text{H}_6$
	+ 0.6	$\text{C}_6\text{H}_6$
	+ 16.9	$\text{C}_6\text{H}_{14}$
	+ 31.7	$\text{C}_6\text{H}_6$
	+ 54.5	$\text{C}_6\text{H}_{14}$
	+119.2	$\text{C}_6\text{H}_{14}$
	+ 86.4	$\text{C}_6\text{H}_{14}$
	+165.3	$\text{C}_6\text{H}_{14}$
	+312.3	$(\text{CH}_3)_2\text{CO}$
	+334.6	$(\text{C}_2\text{H}_5)_2\text{O}$
	+359.4	$(\text{C}_2\text{H}_5)_2\text{O}$
	+377.9	$(\text{C}_2\text{H}_5)_2\text{O}$
	+530.9	$\text{CDCl}_3$

Larger substituent effects are observed for complexes with electronegative groups on the diene system, e.g.  $\text{COOC}_2\text{H}_5$ ,  $\text{COCH}_3$ ,  $\text{CHO}$ , and  $\text{CN}$  groups. These effects become most pronounced when an electronegative atom is directly attached to the metal, as in the series of  $(\eta^3\text{-allyl})\text{Fe}(\text{CO})_3\text{X}$  complexes ( $\text{X} = \text{Cl}, \text{Br}, \text{I}$ ). Schematic spectra are illustrated in Fig. 3. We learn from these data that  $^{57}\text{Fe}$  shielding decreases with increasing electronegativity of the halogen atom and correlates semi-quantitatively with electronegativity values. Further, in the case of the iodo complex, the two stereoisomers, known to be in slow exchange on the NMR time scale, show distinctly different chemical shifts ( $\Delta\nu = 1.56$  KHz at 12.9 MHz). Because of the rather large shift dispersion metal resonances may prove suitable for stereochemical

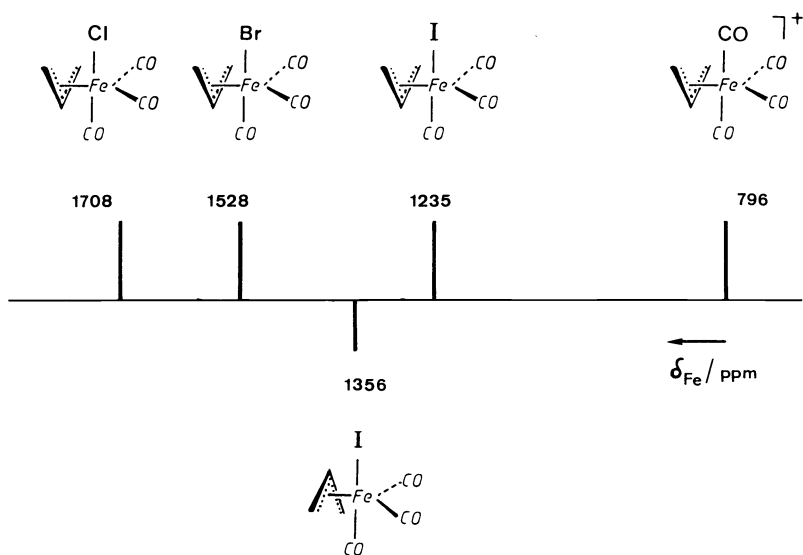
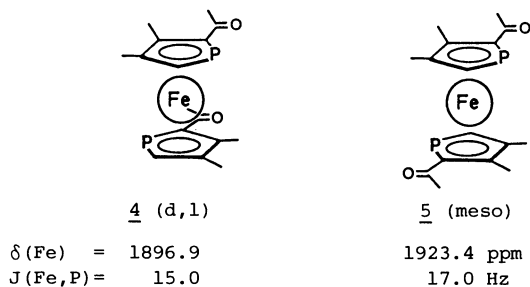


Fig. 3. Schematic  $^{57}\text{Fe}$  spectra of  $(\eta^3\text{-allyl})\text{Fe}(\text{CO})_3\text{X}$  complexes ( $\text{C}_6\text{D}_6$ ) and  $(\text{C}_3\text{H}_5)\text{Fe}(\text{CO})_4\text{BF}_4$  ( $\text{CF}_3\text{COOH}$ ).

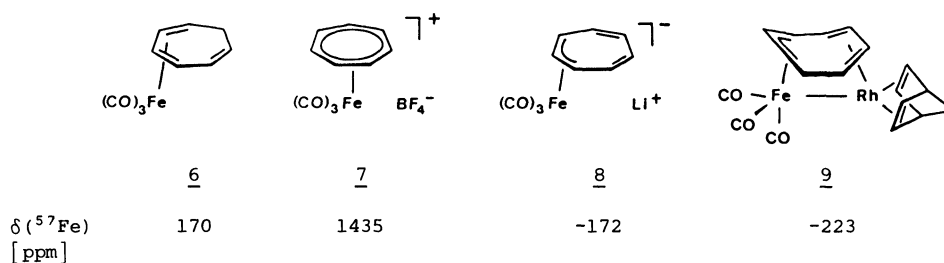
studies. Another example is provided by the diastereomeric diphosphaferrocenes (Note a), the *d,l*-form **4** and the *meso*-form **5** which exhibit a shielding difference of 26.5 ppm. The diastereoisomers were assigned by  $^{31}\text{P}$ -NMR utilizing the chiral shift reagent  $\text{Eu}(\text{hfbc})_3$  which causes a doublet splitting in **4**.

#### Scheme 2





$^{57}\text{Fe}$  chemical shifts have also been used to probe the structure of dinuclear cycloheptatriene and cyclooctatetraene complexes in conjunction with X-ray crystal structures (ref. 14, 1). The shielding data are particularly revealing when both transition metal nuclei, connected by a metal-metal bond, are NMR active as in the case of iron and rhodium. The tricarbonyliron complex of the antiaromatic cycloheptatrienyl anion  $[\text{C}_7\text{H}_7\text{Fe}(\text{CO})_3]\text{Li}$  (**8**) reacts with  $[(\text{norbornadiene})\text{RhCl}]_2$  to form the neutral complex  $\text{Fe}(\text{CO})_3\text{C}_7\text{H}_7\text{RhC}_7\text{H}_7$  (**9**) (ref. 14). The highly shielded  $^{57}\text{Fe}$  resonance of **8** (relative to **6**) is preserved in the dinuclear complex **9** indicating that there is very little, if any, charge transfer from the electron-rich 18e iron atom to the 16e  $\text{Rh}^+$  atom. The latter shows the typical shift of cationic  $\text{Rh}(\text{diene})$  groups which are discussed in the chapter on  $^{103}\text{Rh}$ -NMR. Thus, the dinuclear complex **9** can be justly described as an (18+16)e complex. Further studies of this kind are encouraged involving other metal pairs but it must be emphasized that, as in the present case, chemical shift data of corresponding neutral, cationic and anionic mononuclear complexes must be determined for comparison.

Scheme 3



As mentioned earlier, detection methods for transition metal nuclei may be optimized if the spin-lattice relaxation times are known. Precise data obtained at different field strengths and temperatures are still scarce. In Table 4 we have collected  $T_1$  values for  $^{57}\text{Fe}$  from the Zürich and Tübingen laboratories and data published from other research groups. It is evident that  $T_1$  may vary between 100 s and 10 ms and that only larger molecules exhibit  $T_1$  values below 1 s at ambient temperature. The field dependence is considerable, except for the highly symmetrical iron pentacarbonyl. Dipole-dipole interaction is not effective since no NOE is observable in (diene) $\text{Fe}(\text{CO})_3$  complexes and ferrocene. Therefore, the important relaxation mechanisms for  $^{57}\text{Fe}$  (and other similar spin-1/2 metals) are chemical shift anisotropy ( $B_0^2$  dependent) and nuclear spin rotation. An additional mechanism could be envisaged on the basis of scalar interactions with any paramagnetic species present.

TABLE 4.  $^{57}\text{Fe}$  Spin-lattice relaxation times  $T_1$ /s

Compound	$B_0 = 9.4 \text{ T}$	$2.1 \text{ T a)}$
$\text{Fe}(\text{CO})_5$	67 b)	66 c)
	23 d)	84 e)
	19 f)	88 g)
ferrocene	1.1 h)	3.3 i)
t-butylferrocene	1 k)	4 l) (4.7 T)
carbonmonoxymyoglobin	0.017 m) (8.45 T)	-

a)  $T_1$  values at 2.1 T were determined by Dr. A. Schwenk (Tübingen); b) 6.4 M in  $\text{C}_6\text{D}_6$ , 297 K; at 7.1 T and 293 K ( $\text{C}_6\text{D}_6$ ) a value of  $80 \pm 10$  s was reported (ref. 15); c) as b), 300 K; d) 4.4 M in  $\text{C}_6\text{D}_6$ , 295 K; e) as d), 300 K; f) 3.8 M in  $\text{C}_6\text{D}_6$ , 295 K; g) as f), 300 K; h) 1.3 M in  $\text{CDCl}_3$ , 295 K; i) as h), 300 K; k) 80% acetone- $d_6$ , 298 K (ref. 16); l) as k); m) 0.015 M in  $\text{H}_2\text{O}$ , pH 7.1, 296 K (ref. 17).

To date, only a small number of iron chemical shifts of complexes with the metal in higher oxidation states have been reported. They include iron(II) porphyrin complexes of biological importance (ref. 16, 18) and the protein carbonmonoxymyoglobin (ref. 17) showing highly deshielded resonances in the range from 7000 to 9000 ppm. Complexes of this size exhibit very short spin-lattice relaxation times (Table 4) which facilitates measurement of the metal resonance. On the other hand, difficulties may arise if paramagnetic species (Fe(III)) are also involved. Nevertheless, it can be expected that in the

future the extremely rich organometallic chemistry and biochemistry of iron will be supported by  $^{57}\text{Fe}$  NMR studies.

### $^{103}\text{Rh}$ -NMR Studies

Earlier investigations of rhodium chemical shifts were conducted by indirect  $^1\text{H}$ - $\{^{103}\text{Rh}\}$  or  $^{13}\text{C}$ - $\{^{103}\text{Rh}\}$  double resonance experiments (ref. 12) which are facilitated by the 100% natural isotope abundance and sizable Rh,X spin coupling constants, particularly in rhodium hydride complexes. Direct observations at low and medium field strengths (ref. 19) were handicapped by excessive measuring times. The first systematic study of CpRh(diene) complexes was carried out using direct steady state pulse techniques (ref. 20,5). The relatively favorable receptivity, 45 times higher than  $^{57}\text{Fe}$ , and the large chemical shift range (10'000 ppm) (Fig. 4) render this metal nucleus

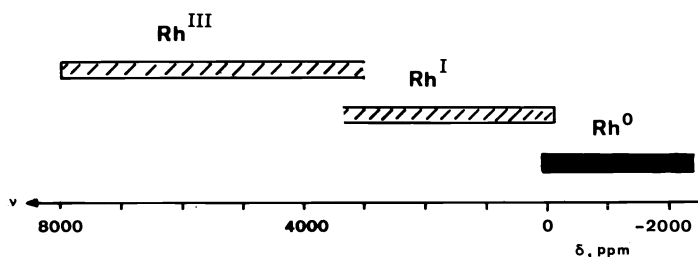


Fig. 4. Chemical shift ranges for rhodium compounds,  $\delta$  values rel. to  $\nu(\text{Rh}) = 3.16$  MHz.

an excellent probe to support the structures of mono- and dinuclear complexes, and even rhodium clusters. The remaining obstacle, rather long  $T_1$  values, is largely overcome since high-field spectrometers have been used ( $B_0 = 9.4$  T,  $\nu(\text{Rh}) = 12.6$  MHz) (ref. 21, 22, 23). Under these conditions,  $T_1(\text{Rh})$  is in the range of 1-10 sec. for CpRh(diene) complexes, and larger molecules have  $T_1$  values  $< 1$  sec.

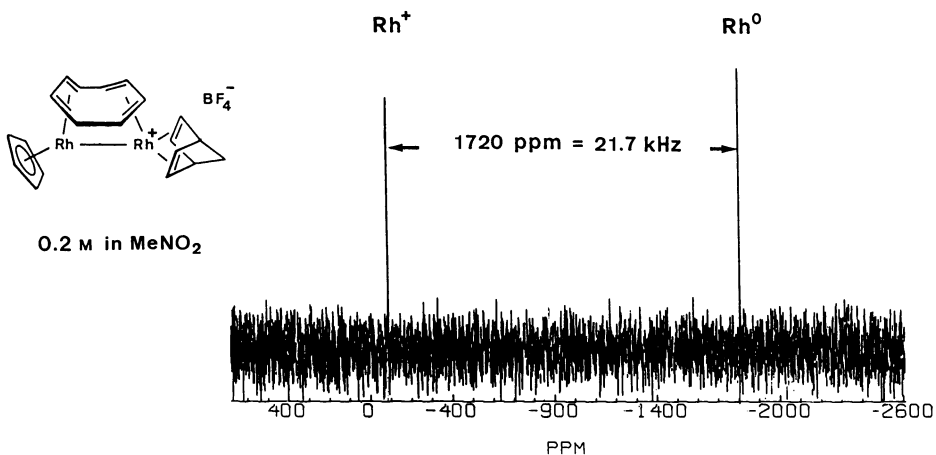


Fig. 5.  $^{103}\text{Rh}$ -NMR spectrum of  $[\text{CpRh}(\text{COT})\text{Rh}(\text{NBD})]\text{BF}_4$ , 12.6 MHz, 10 mm tube, total acquisition time 38 min.

A typical spectrum (Fig. 5) shows the large shielding difference (1720 ppm) of the Rh(0) and Rh(I) atoms in  $[\text{CpRh}(\text{COT})\text{Rh}(\text{NBD})]\text{BF}_4$ . This result when compared with chemical shifts of mononuclear CpRh(diene) complexes (-2050 to -350 ppm) and (acac)Rh(diene) complexes (+1180 to +1760 ppm) or Rh(I)X(COD) complexes (X = Cl, OMe: +1100 to +1300 ppm) has induced us to assign the (formal) oxidation state zero to CpRh moieties. It is interesting to note



that the Rh(0) and Rh(I) species are preserved in the dinuclear complex despite the presence of a weak Rh-Rh bond (296.2 pm), so that this complex may be described as another (18+16)e system, just as in the case of complex 9.

The characteristic influence of diene geometry on the metal chemical shift, already described in the iron series, is also observed in CpRh(diene) complexes (Fig. 6).

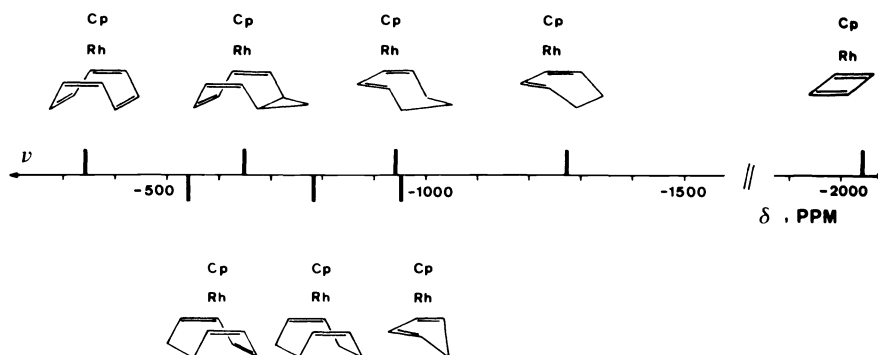
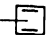
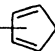
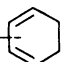
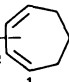


Fig. 6.  $^{103}\text{Rh}$  chemical shift range of CpRh(diene) complexes,  $\delta(\text{ppm})$  rel. to  $\nu(\text{Rh}) = 3.16$  MHz.

Here, the stereoelectronic effect is further reflected in the one-bond  $^{103}\text{Rh}$ ,  $^{13}\text{C}$  coupling constants (Table 5) which increase for the terminal carbons of the 1,3-diene system with increasing ring size. Thus, the s-character of the carbon orbital in the Rh,C bond increases due to  $(\text{sp}^2, \text{p}) \rightarrow \text{sp}^3$  rehybridization. At the same time, Rh,C coupling involving the central C-atoms of the diene decreases. The overall change in carbon orbital overlap with the rhodium d-orbitals leads to metal deshielding.

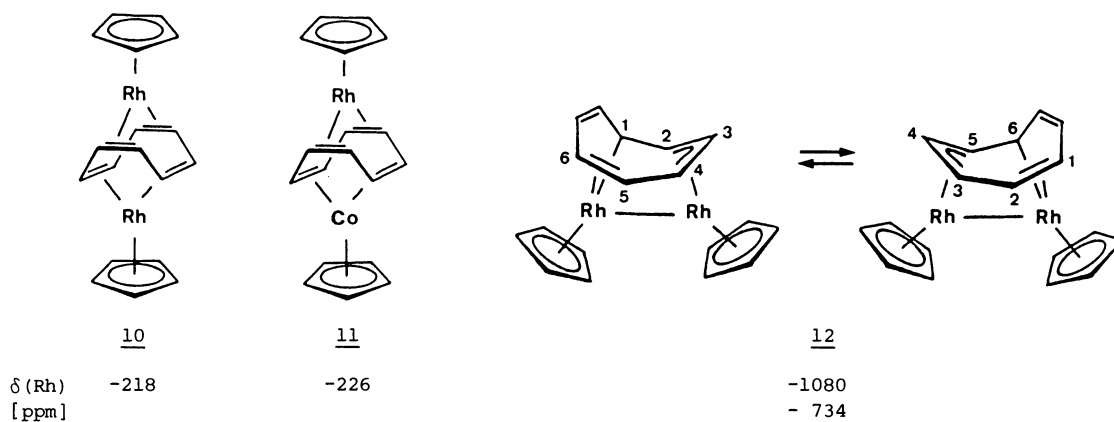
TABLE 5.  $^1\text{J}(\text{Rh}, \text{C})$  coupling constants [Hz]

	C(1)	C(2)
Cp Rh 	11.7	11.7
Cp Rh 	11.9	9.4
Cp Rh 	15.4	7.3
Cp Rh 	17.4	6.1

An extensive study of 16-electron Rh(I)X(COD) complexes (X = O, N, Cl, Br, I) was carried out by Bonnaire et al. (ref. 22). The results have confirmed that the range of Rh(I) resonances (+350 to +1750 ppm) excludes the 18-electron pure olefin complexes CpRh(diene) in which the Rh nucleus is more shielded by 1000 - 3000 ppm. Steric effects leading to high-frequency shifts of the Rh resonance have also been observed in the above Rh(I) series where  $\delta(\text{Rh})$  has been correlated with various ligand properties and  $\delta(^{13}\text{C})$  and  $^1\text{J}(\text{Rh}, \text{P})$  data.

Rh-NMR was successfully applied to support the structures of the isomeric dinuclear complexes  $(\text{CpRh})_2\text{COT}$  (10) and (12), formed in the reaction of  $[(\text{COT})\text{RhCl}]_2$  with CpTl at 25° and -80°, respectively (ref. 1, 24):

Scheme 4



The yellow symmetrical *trans*-complex 10 shows one  $^{103}\text{Rh}$  signal at -218 ppm, in agreement with  $\eta^4$ -1,2:5,6-coordination (CpRhCOT: -348 ppm) whereas in the red complex 12, despite its fluxional structure, the two Rh atoms are non-equivalent and more shielded, one Rh atom always being  $\eta^3(\sigma, \pi)$ - and the other  $\eta^3(\pi\text{-allyl})$ -coordinated. While the  $^{13}\text{C}$  spectrum of eight ring carbons is temperature-dependent (i.e. 4 resonances at 25°, 8 at -70°), the two-line Rh spectrum and the  $^{13}\text{C}$  resonances of the Cp units are not, thus supporting the indicated fluxional process first observed in the analogous structure of CpRh(1-6- $\eta$ -cyclooctatriene)RhCp (ref. 25). In the *trans*-complex 11 one of the RhCp units is replaced by CpCo without a significant influence on the Rh chemical shift (-226 ppm), which is in agreement with the orthogonal arrangement of the two diolefin systems of the bis-1,5-coordinated COT ligand.

Rh-NMR was further applied to rhodium clusters (ref. 26, 27, 28), and the results have shown that both charge separation and rhodium atom fluxionality can be demonstrated. As an example for the latter, the variable-temperature  $^{103}\text{Rh}$  spectra of the cluster anion  $[\text{Rh}_9\text{P}(\text{CO})_{21}]^{2-}$  are illustrated in Fig. 7 (ref. 26a). In the slow-exchange limit at 183 K, three resonances (1:4:4)

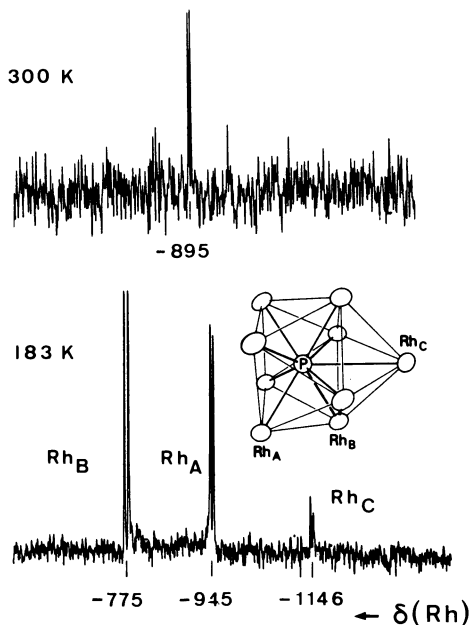


Fig. 7.  $^{103}\text{Rh}$ -NMR spectra and metal atom skeletal structure of the  $[\text{Rh}_9\text{P}(\text{CO})_{21}]^{2-}$  anion,  $(\text{CD}_3)_2\text{CO}$ , 5.7 MHz,  $\delta(\text{Rh})$  rel. to the  $[\text{Rh}_6\text{C}(\text{CO})_{15}]^{2-}$  ion, from ref. 26a.

are observed with a doublet splitting due to coupling with the central phosphorus atom, the result being supported by the crystal structure.

As yet, no direct applications of  $^{103}\text{Rh}$ -NMR to studies of nuclear systems relevant to homogeneous catalysis have become known. However, it will be shown in the subsequent chapter that the investigation of substituted  $\text{CpCo}(\text{diolefin})$  complexes has revealed systematic structural effects on the  $^{59}\text{Co}$  resonance, which have been successfully applied in correlations with and predictions of the activity and regioselectivity of homogeneous catalysts.

### $^{59}\text{Co}$ -NMR Studies

Organocobalt complexes with the metal in low-valent oxidation states have become of considerable importance as catalysts in organic synthesis (ref. 29, 30). On the other hand, extensive investigations of  $^{59}\text{Co}$  chemical shifts have so far been focussed on quasi-octahedral  $\text{Co}(\text{III})$  complexes or cobalt carbonyl complexes (ref. 12). Until 1983, only a few experimental data have become known of organo-cobalt compounds in the low-frequency range (high shielding) of the total chemical shift scale of  $^{59}\text{Co}$  (Fig. 8) which extends over 18'000 ppm, i.e.  $\sim 1.7$  MHz at a detecting frequency of 94.5 MHz (9.4 T).

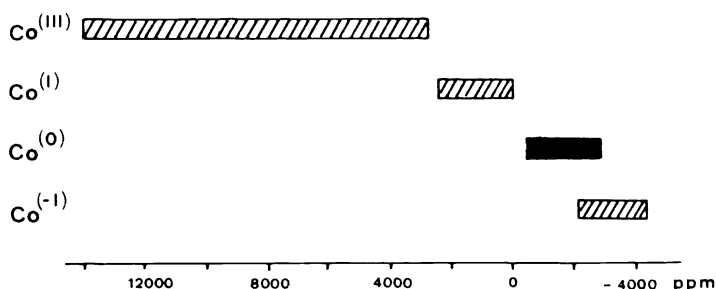


Fig. 8. Total chemical shift range of cobalt compounds,  $\delta(\text{Co})$  rel. to  $\text{K}_3[\text{Co}(\text{CN})_6]$ .

The reason for this fact lies in the large  $^{59}\text{Co}$ -NMR line width (5-30 KHz) associated with complexes of low symmetry and high molecular weight due to large electric field gradients and slow molecular tumbling, respectively. The very short relaxation times, however, permit rapid pulsing and thus, together with the high receptivity of this nucleus (Table 1), an efficient detection even in dilute solutions. Modern high-field multinuclear spectrometers can handle line widths up to 35 KHz and, therefore, the systematic investigation of cobalt(olefin) complexes becomes feasible. We have recently studied a variety of  $\text{CpCo}(\text{diolefin})$  complexes which cover a chemical shift range of more than 2000 ppm (ref. 24, 31). Since this topic is subject of a separate communication at this conference (ref. 31b), we will only outline a few important findings and then discuss their application to homogeneous catalysis.

It is important to realize that  $^{59}\text{Co}$  chemical shifts and line widths, like those of other transition metal resonances, are solvent- and temperature-dependent. An interpretation of these parameters should, therefore, be based on data obtained under comparable conditions. It may be advantageous in some cases to increase solvent polarity and temperature to reduce the experimental line width if the  $^{59}\text{Co}$  resonance is detected only with difficulty. Figure 9 illustrates  $^{59}\text{Co}$  signals of two typical olefin complexes. In Fig. 10, the line widths of two low-valent cobalt complexes are shown as a function of temperature.  $\delta(\text{Co})$  values can usually be determined with an accuracy of  $\pm 5$ -15 ppm for line widths of 5-30 KHz. The temperature coefficients are of the order of +1 ppm/K (ref. 24). Chemical shifts are referred to  $\text{K}_3[\text{Co}(\text{CN})_6]$  as an external standard which yields a sharp resonance line.

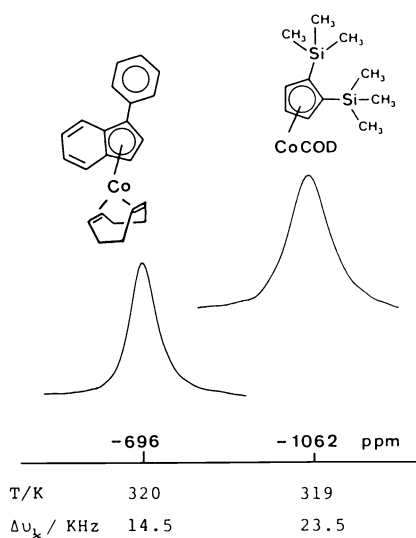


Fig. 9.  $^{59}\text{Co}$  spectra (94.5 MHz) of two typical low-valent cobalt(olefin) complexes, in  $\text{C}_6\text{D}_6$ ,  $\delta(\text{Co})$  rel. to  $\text{K}_3[\text{Co}(\text{CN})_6]$ .

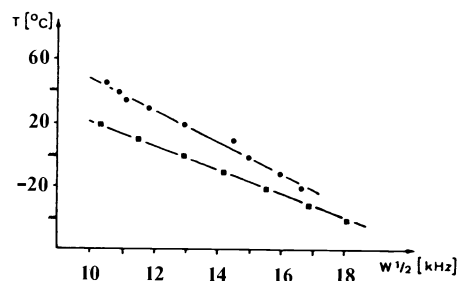
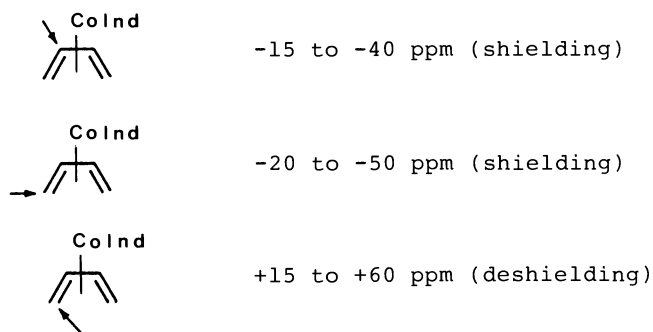


Fig. 10.  $^{59}\text{Co}$ -NMR line widths of  $\text{CpCo}(\text{CO})_2$  (■) and  $\text{CpCo}(\text{bicyclo}[4.2.0]\text{octa-1,3-diene})$  (●) in acetone as a function of temperature (ref. 24).

$^{59}\text{Co}$  chemical shifts of  $\text{CpCo}$  moieties,  $\eta^4$ -complexed with cyclic or non-cyclic dienes, extend over a range of 2200 ppm, corresponding to more than 10% of the total shift scale of this nucleus (Fig. 8). They are, therefore, sensitive to details of ligand structure and coordination, and some trends are as follows:

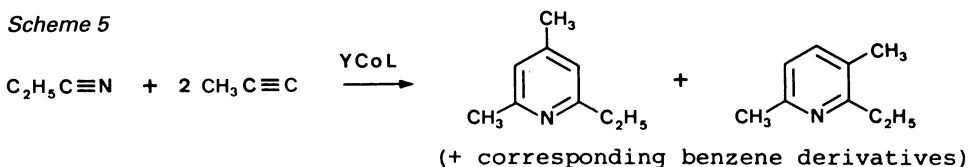
- 1) 1-4- $\eta$ -diene complexes show the highest shielding, i.e. in the range from -2900 ppm to -1270 ppm.  
1,2:4,5-diene complexes are less shielded, i.e. from -1370 to -1010 ppm.  
1,2:5,6-systems appear at the highest frequency, i.e. from -1140 ppm to -600 ppm.
- 2) Within the group of 1-4- $\eta$ -diene complexes shielding decreases with increasing ring size, i.e., with increasing C,C,C-bond angle.
- 3) Within the group of 1,2:5,6-dienes, further conjugation of the 1,5-diene system leads to a high-frequency shift.
- 4) Methyl substituents on the open-chain 1-4- $\eta$ -butadiene ligand have a rather complex influence:



- 5) Substitution of the cyclopentadienyl moiety by  $\eta^5$ -indenyl gives a strong high-frequency shift (+350 ppm).
- 6) Substitution at the cyclopentadienyl moiety by electron-withdrawing or electron-donating substituents causes systematic shifts towards high and low-frequency, respectively.

It should be noted that similar trends in the shielding of low-valent metal (diolefin) systems are observed for Co, Rh and Fe complexes. It is also of interest with regard to homogeneous catalysis by cobalt complexes that the thermally less stable 1,2:5,6- $\eta$ -complexes are strongly deshielded relative to the less reactive 1-4- $\eta$ -complexes, in particular CpCo(cyclobutadiene) which cannot be thermally activated < 200° (ref. 32). Further  $^{59}\text{Co}$ -NMR data on organo-cobalt complexes, including ( $\eta^3$ -allyl) $_3\text{Co}$  systems, have recently been reported by Benn et al. (ref. 34).

At this point of our investigations on the  $^{59}\text{Co}$  resonance in olefin complexes, we had the good fortune to come into close contact with the research group of Prof. H. Bönemann (MPI Mülheim) who is engaged in the Co-catalyzed synthesis of pyridine derivatives from acetylenes and nitriles (ref. 30). Subsequent work in the Zürich and Mülheim laboratories has revealed excellent correlations of  $^{59}\text{Co}$  shielding values with catalytic data obtained in a continuous flow reactor (ref. 32, 33, 30). At present, the correlations include over 30 active catalysts of the CpCo(COD) and (indenyl)Co(COD) types, the catalytic activity being determined under standardized conditions using the test reaction



Under standardized concentration conditions for educts and catalysts the temperature was determined at which 65% of the propyne is transformed continuously to products. This temperature value is a good measure for the activity of the Co catalyst, and correlations of  $T$  with  $\Delta\delta(\text{Co})$  for R-CpCo(COD) and (R-indenyl)Co(COD) complexes are given in Figs. 11 and 12. It is clear that highly active catalysts with a low reaction temperature are associated

$$T[^\circ] = 160.6 - 0.25 \cdot \Delta\delta(\text{Co})$$

$$T[^\circ] = 131.6 - 0.17 \cdot \Delta\delta(\text{Co})$$

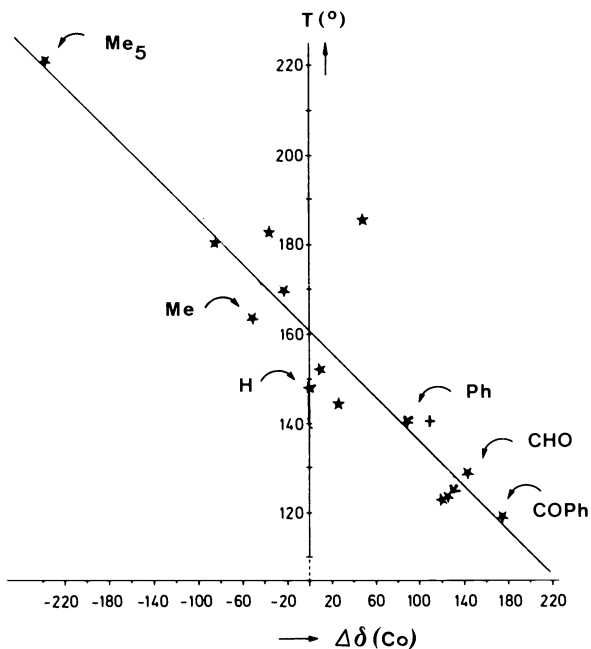


Fig. 11. Catalytic activity of R-CpCo (COD) complexes as a function of the  $^{59}\text{Co}$  chemical shift (reaction temperatures under standard conditions in the test reaction of Scheme 5 (ref. 30, 32)).

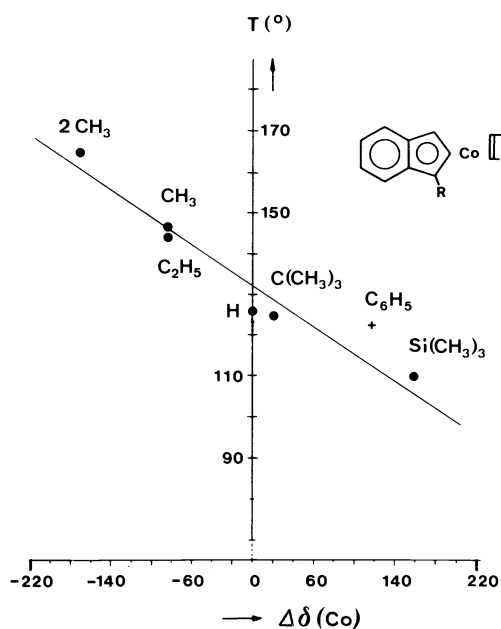


Fig. 12. Analogous correlation diagram for (R-indenyl)Co(COD) complexes (regression analysis without phenyl data).

with a deshielded Co resonance (i.e. high-frequency shift, large positive  $\Delta\delta(\text{Co})$ -value). The quality of these correlations (high  $r$ -values) and the relatively large chemical shift range ( $\sim 400$  ppm) suggest a promising novel technique for an efficient screening of homogeneous catalysts.

A second type of correlation of  $^{59}\text{Co}$  shifts was obtained with the regioselectivity of the catalysts (Fig. 13). Clearly, the active catalysts with deshielded  $^{59}\text{Co}$  signals are less selective with respect to the ratio of sym./unsym. products (Scheme 5) than the highly shielded and less reactive representatives.

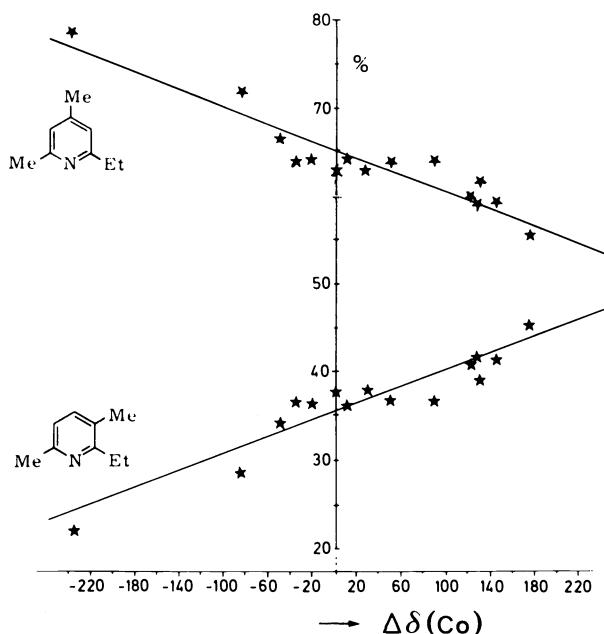


Fig. 13. Regioselectivity of  $\text{RCpCo}(\text{COD})$  complexes as a function of the  $^{59}\text{Co}$  chemical shift (rel. yields of sym. and unsym. product according to Scheme 5).

The basis for these novel correlations between a metal chemical shift and catalytic activity is given by the fact that the substituent effects observed in the  $^{59}\text{Co}$  resonance of the pre-catalyst  $\text{RCpCo}(\text{COD})$  are also effective in the catalytically active species  $\{\text{RCpCo}\}$  since the  $\text{RCp}$  moiety remains attached to the cobalt centre throughout the catalytic cycle. Practical limitations of this catalyst screening method are set by the excessive  $^{59}\text{Co}$  line width of larger catalyst molecules (cf. Fig. 9) or solubility problems in the flow reactor.

An attractive extension of the application of  $^{59}\text{Co}$ -NMR to chemical reactivity can be envisaged in biocatalysis using cobalamins (vitamin- $\text{B}_{12}$  derivatives). Preliminary experiments in our laboratory, in collaboration with Dr. B. Kräutler (ETH-Zürich), have shown that the molecular size of these complexes is not a limiting factor in obtaining  $^{59}\text{Co}$  shielding data. As an illustration the  $^{59}\text{Co}$  spectra of vitamin  $\text{B}_{12}$  (cyanocobalamin) and methylcobalamin are depicted in Fig. 14. The high sensitivity of detection allows the study of rather dilute solutions (millimolar), and the line-width can be reduced sufficiently at temperatures above 300 K.

An early study (1969) of the  $^{59}\text{Co}$  resonance of vitamin  $\text{B}_{12}$  model compounds (ref. 35) has already provided evidence that the chemical shifts are largely determined by the Co nearest neighbor heteroatoms. With a constant template of four equatorial N-ligands a variation in  $\delta(\text{Co})$  is expected to be caused mainly by the nature of the axial ligands. Substitution of CN by methyl produces the expected low-frequency shift ( $\Delta\delta(\text{Co}) \sim -500$  ppm) in the spectrum of the methylcobalamin. Further applications to structural chemistry and catalysis of cobalamins are in progress.

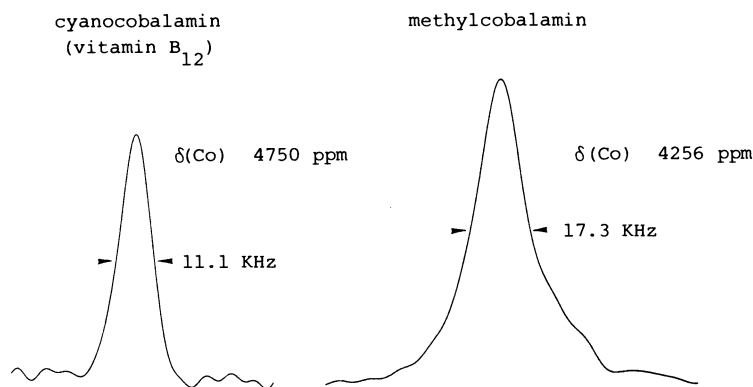


Fig. 14.  $^{59}\text{Co}$ -NMR spectra (94.9 MHz) of cyanocobalamin (vitamin B<sub>12</sub>, D<sub>2</sub>O, 0.01 M, total acquisition time 10 s) and methylcobalamin (D<sub>2</sub>O, 0.02 M, total acquisition time 47 s);  $\delta(\text{Co})$  rel. to  $\text{K}_3[\text{Co}(\text{CN})_6]$ .

## CONCLUSIONS

Despite the inherent experimental difficulties associated with NMR spectroscopy of transition metals many of the chemically relevant nuclei have recently found increasing attention from spectroscopists, organometallic chemists and biochemists. Some important metals, e.g. non-symmetrically coordinated Pd and Ni, have still proven rather elusive, and further improved detection techniques are desirable for an investigation of their spectral parameters in a wider sense. The large chemical shifts of transition metal nuclei and their sensitivity to structural changes permit various applications in structural and mechanistic organometallic chemistry. Examples, which have been investigated to date, range from mono-nuclear olefin complexes of low-valent metals to cluster compounds, metal-protein complexes, and homogeneous catalysts, including bio-catalysts. With respect to a systematic investigation of the structural factors influencing chemical shifts, heteronuclear and homonuclear spin coupling and relaxation times, transition metal NMR is still in its infancy and comparable to proton or carbon-13 spectroscopy in the 1960s and 1970s, respectively. The great potential of this third generation of nuclei for NMR studies of chemical structure and reactivity, however, is already clearly discernible.

## Acknowledgements

The author wishes to express gratitude and indebtedness to his coworkers who have contributed to the results presented in this survey, i.e. Dr. T. Jenny, Dr. T. Egolf, A. Hafner, K. Täschler, U. Piantini, C. Adams, Dr. R.W. Kunz, and Dr. R. Hollenstein. Over the years, the Zurich laboratory has enjoyed the cooperation of Dr. A. Schwenk, University of Tübingen, who has assisted and supported our studies with expertise and enthusiasm. In many of the synthetic and structural studies the collaboration with Dr. A. Salzer and his research group has been essential. Generous financial support by the Zurich Government and the Swiss National Science Foundation is gratefully acknowledged.

## REFERENCES

1. J.H. Bieri, T. Egolf, W. von Philipsborn, U. Piantini, R. Prewo, U. Ruppli and A. Salzer, *Organometallics*, in preparation.
2. C.J. Turner, *Prog. Nucl. Magn. Reson. Spectrosc.*, **16**, 311-370 (1984); C. Brevard and R. Schimpf, *J. Magn. Reson.*, **47**, 528-534 (1982); A. Costa, M. Tato and R.S. Matthews, *Magn. Reson. Chem.*, in preparation.
3. A. Schwenk, *Prog. Nucl. Magn. Reson. Spectrosc.*, in press; A. Schwenk, *J. Magn. Reson.*, **5**, 376-389 (1971), **37**, 551-553 (1980); J. Kronenbitter and A. Schwenk, *ibid*, **25**, 147-165 (1977).
4. a) T. Jenny, W. von Philipsborn, J. Kronenbitter and A. Schwenk, *J. Organomet. Chem.*, **205**, 211-222 (1981); b) A. Schwenk, *Phys. Letters*, **31A**, 513-514 (1970).

5. E. Maurer, S. Rieker, M. Schollbach, A. Schwenk, T. Egolf and W. von Philipsborn, Helv. Chim. Acta, **65**, 26-45 (1982).
6. G.A. Morris and R. Freeman, J. Am. Chem. Soc., **101**, 760-762 (1979).
7. D.M. Doddrell, D.T. Pegg and M.R. Bendall, J. Magn. Reson., **48**, 323-327 (1982); D.T. Pegg, D.M. Doddrell and M.R. Bendall, J. Chem. Phys., **77**, 2745-2752 (1982).
8. K. Bachmann and W. von Philipsborn, Org. Magn. Reson., **8**, 648-654 (1976).
9. S. Ruh and W. von Philipsborn, J. Organomet. Chem., **127**, C59 (1977); S. Zobl-Ruh and W. von Philipsborn, Helv. Chim. Acta, **63**, 773-779 (1980), **64**, 2378-2382 (1981).
10. A.A. Koridze, P.V. Petrovskii, S.P. Gubin and E.I. Fedin, J. Organomet. Chem., **93**, C26-30 (1975); A.A. Koridze, N.M. Astakhova and P.V. Petrovskii, J. Organomet. Chem., **254**, 345-360 (1983).
11. E. Haslinger, K. Koci, W. Robin and K. Schlögl, Monatsh. Chem., **114**, 495-499 (1983); E. Haslinger, W. Robin, K. Schlögl and W. Weissensteiner, J. Organomet. Chem., **218**, C11-14 (1981).
12. cf. R. Garth Kidd and R.J. Goodfellow in: "NMR and the Periodic Table", R.K. Harris and B.E. Mann, Eds., Academic Press 1978, p. 225-249.
13. A. Hafner and W. von Philipsborn, Magn. Reson. Chem., in preparation; A. Hafner, PhD Thesis, University of Zürich, 1986.
14. A. Salzer, T. Egolf and W. von Philipsborn, Helv. Chim. Acta, **65**, 1145-1157 (1982).
15. T. Nozawa, M. Hatano, M. Sato, Y. Toida and E. Batholdi, Bull. Chem. Soc. Jpn., **56**, 3837-3838 (1983).
16. L. Baltzer, E.D. Becker, B.A. Averill, J.M. Hutchinson and O.A. Gansow, J. Am. Chem. Soc., **106**, 2444-2446 (1984).
17. H.C. Lee, J.K. Gard, T.L. Brown and E. Oldfield, J. Am. Chem. Soc., **107**, 4087-4089 (1985).
18. T. Nozawa, M. Sato, M. Hatano, N. Kobayashi and T. Osa, Chem. Lett. **1983**, 1289.
19. D.S. Gill, O.A. Gansow, F.J. Bennis and K.C. Ott, J. Magn. Reson., **35**, 459-461 (1979).
20. K.D. Grüniger, A. Schwenk and B.E. Mann, J. Magn. Reson., **41**, 354-357 (1980).
21. M. Cocivera, G. Ferguson, R.E. Lenkinski, P. Szczecinski, F.J. Lalor and D.J. O'Sullivan, J. Magn. Reson., **46**, 168-171 (1982).
22. R. Bonnaire, D. Davoust and N. Platzler, Org. Magn. Reson., **22**, 80-85 (1983).
23. B.E. Mann and C.M. Spencer, Inorg. Chim. Acta, **65**, L57-58 (1982); **76**, L65-66 (1983).
24. T. Egolf, PhD Thesis, University of Zürich, 1983.
25. J. Evans, B.F.G. Johnson, J. Lewis and R. Watt, J. Chem. Soc. Dalton **1974**, 2368-2374.
26. a) O.A. Gansow, D.S. Gill, F.J. Bennis, J.R. Hutchinson, J.C. Vidal and R.C. Schoening, J. Am. Chem. Soc., **102**, 2449-2450 (1980);  
b) C. Brown, B.T. Heaton, L. Longhetti, D.O. Smith, P. Chini and S. Martinengo, J. Organomet. Chem., **169**, 309-314 (1979).
27. L. Garlaschelli, A. Fumagalli, S. Martinengo, B.T. Heaton, D.O. Smith and L. Strona, J. Chem. Soc. Dalton **1982**, 2265-2267; B.T. Heaton, L. Strona, R. Della Pergola, L. Garlaschelli, N. Sartorelli and I.H. Sadler, J. Chem. Soc. Dalton **1983**, 173-175.
28. G. Schmid, U. Giebel, W. Huster and A. Schwenk, Inorg. Chim. Acta, **85**, 97-102 (1984).
29. K.P.C. Vollhardt, Angew. Chem., **96**, 525-541 (1984); Angew. Chem. Int. Ed., **23**, 539-555 (1984).
30. H. Bönemann, Angew. Chem., **97**, 264-279 (1985); Angew. Chem. Int. Ed., **24**, 248-263 (1985).
31. a) C. Täschler, T. Egolf and W. von Philipsborn, Helv. Chim. Acta, in preparation; b) *idem*, cf. Abstracts of Poster presentations at XII Int. Conf. Organomet. Chem. Vienna, 1985.
32. H. Bönemann, W. Brijujoux, R. Brinkmann, W. Meurers, R. Mynott, W. von Philipsborn and T. Egolf, J. Organomet. Chem., **272**, 231-249 (1984).
33. W. Meurers, PhD Thesis, Techn. Hochschule Aachen, 1985.
34. R. Benn, K. Cibura, P. Hofmann, K. Jonas and A. Rufinska, Organometallics, in preparation.
35. H.A.O. Hill, K.G. Morallee, G. Costa, G. Pellizer and A. Loewenstein in: "Magn. Resonances Biol. Res.", Rep. 3rd Int. Conf. 1969, C. Franconi, Ed., Gordon & Breach, New York 1971, p. 301.